Journal of Hepatocellular Carcinoma

Dovepress
open access to scientific and medical research

Open Access Full Text Article

ORIGINAL RESEARCH

Effect of Inhibiting Tumor Angiogenesis After Embolization in the Treatment of HCC with Apatinib-Loaded p(*N*-Isopropyl-Acrylamide-*co*-Butyl Methyl Acrylate) Temperature-Sensitive Nanogel

This article was published in the following Dove Press journal:
Journal of Hepatocellular Carcinoma

Chen Zhou[1,2,*]
Qin Shi[1,2,*]
Jiacheng Liu[1,2]
Songjiang Huang[1,2]
Chongtu Yang[1,2]
Bin Xiong[1,2]

[1]Department of Radiology Union Hospital Tongji Medical College, Huazhong University of Science and Technology, Wuhan, Hubei, 430022, People's Republic of China; [2]Hubei Province Key Laboratory of Molecular Imaging, Wuhan, Hubei, 430022, People's Republic of China

*These authors contributed equally to this work

Background: Transcatheter arterial embolization (TAE) is widely used in hepatocellular carcinoma (HCC) therapy. Tumor hypoxia often correlates with the recurrence and metastasis of the tumor and is the critical factor limiting the treatment effect of TAE.

Purpose: To investigate the underlying mechanism and therapeutic potential of TAE combined with apatinib-loaded p(*N*-isopropyl-acrylamide-*co*-butyl methyl acrylate) temperature-sensitive (PIB) nanogel for the suppression of rabbit VX2 liver tumor growth.

Materials and Methods: Sixty-five VX2 tumor-burdened rabbits were randomly divided into five groups and treated transarterially with apatinib-loaded PIB (Group PA, 0.4 mL, n=13), PIB alone (Group P, 0.4 mL, n=13), iodized oil alone (Group I, 0.4 mL, n=13), apatinib solution (Group A, 0.4 mL, n=13) or saline (Group NS, 0.4 mL, n=13). The dose of apatinib was 2 mg/kg. Tumors were harvested, sectioned and immunohistochemically stained, and the tumor growth rates and survival times in each group were measured. Blood samples and liver tissues were collected for pharmacokinetic analysis.

Results: The tumor growth rate in Group PA was considerably lower than the other four groups ($P=0.000<0.01$), and the survival time was significantly prolonged ($P=0.000<0.01$). The immunohistochemistry results showed that CD31 expression was significantly lower in Group PA than that of the other four groups ($P=0.000<0.01$). The apatinib concentration in the blood fell below 10 ng/mL within 10 min after TAE and dropped below 1 ng/mL after 8 h. The drug was released continuously in the liver for 36 days, with the highest concentration at the tumor junction ($P=0.045<0.05$).

Conclusion: PIB effectively targeted apatinib to HCC tissues, achieved a slow and sustained release of the drug in the tumor and considerably reduced the systemic drug concentration. Further experiments showed significantly prolonged survival times and an inhibitory effect on tumor growth.

Keywords: HCC, transcatheter arterial embolization, tumor angiogenesis, apatinib, PIB

Correspondence: Bin Xiong
Department of Radiology, Union Hospital, Tongji Medical College, Huazhong University of Science and Technology, 13 Aviation Road, Wuhan, 430022 Hubei, People's Republic of China
Tel +86 13720321015
Email herr_xiong@126.com

Introduction

Hepatocellular carcinoma (HCC) mortality ranks third among global cancer deaths.[1–3] Transcatheter arterial embolization (TAE) is widely used in the intermediate stage HCC therapy.[4] However, two main factors limit the long-term effects of TAE. First, HCC angiogenesis induced by hypoxia in the tumor after TAE has been shown to play a crucial role in promoting the malignant biological behavior of

HCC. Second, the embolization of tumor peripheral blood vessels can also be a key factor affecting the curative impact of TAE.[5,6] Therefore, it is critically essential to identify new therapeutic strategies for HCC.

HCC is a blood-rich tumor, and therefore malignant angiogenesis is the most significant abnormally activated pathway in HCC progression.[7–9] In HCC, TAE exacerbates ischemia and hypoxia, resulting in the persistent excess of vascular endothelial growth factor (VEGF).[10–12] The combination of VEGF and VEGF receptor (VEGFR) triggers a cascade of downstream pathways, which eventually induces tumor neovascularization, resulting in tumor recurrence and metastasis.[13,14] Moreover, tumor neovascularization causes abnormal leakage of blood vessels, which can lead to the development of edema, interstitial hypertension and further aggravate hypoxia in HCC, forming a vicious cycle of hypoxia, HCC growth and nonproductive angiogenesis after TAE.[12,15,16] VEGFR2 plays a significant role in mediating the angiogenesis driven by VEGF.[17,18] Accordingly, inhibiting the VEGF/VEGFR signaling pathway that involves VEGFR2 can disrupt this vicious circle, thereby preventing the neovascularization of HCC after TAE treatment, reducing the recurrence and metastasis of HCC and improving the short- and long-term efficacy of TAE treatment.[19–26] Therefore, it is of considerable significance to develop effective drugs and treatment methods to inhibit the recurrence and metastasis of HCC.

As a single-target inhibitor of VEGFR2, apatinib mesylate can efficiently inhibit tumor angiogenesis.[27,28] Apatinib exhibits antitumor and anti-angiogenic activities in several cancers, including colon, non-small cell lung, breast and gastric and others.[29–33]

Embolization materials play a crucial role in TAE.[34] At present, the commonly used embolization agents, such as gelatin sponge particles, polyvinyl alcohol particles, liquid lipiodol, and drug-eluting microspheres, all have certain shortcomings.[35–44] We previously developed and performed a series of studies on poly(*N*-isopropyl acrylamide-*co*-butyl methyl acrylate) temperature-sensitive (PIB) nanogel. We confirmed that PIB nanogel is safe and effective and has excellent biocompatibility, strong controllability and accessible operation embolization agent.[38,45–47]

In this study, apatinib-loaded PIB nanogels were explored for the first time as TAE therapy in HCC. We monitored treatment responses and survival times, and we used imaging, immunology and pathology methods to evaluate the effectiveness and safety of embolization. Additionally, given our limited understanding of the pharmacokinetic changes before and after TAE with apatinib-loaded PIB nanogel, we performed an in-depth study to clarify the pharmacokinetics of apatinib in HCC models. Overall, this study was designed to explore new strategies for the interventional treatment of HCC.

Methods and Materials

Materials

PIB nanogels were prepared by emulsion polymerization in accordance with previously published methods.[47] *N*-isopropyl acrylamide (NIPAM, Tokyo Chemical Industry, Japan) and *N*,*N*-methylenebisacrylamide (BIS, Kermel Chemical Industry, China) were respectively recrystallized from n-hexane and methanol. API 4000 triple quadrupole mass spectrometer (AB Company, USA) equipped with electrospray ionization source, XW-80A Vortex Mixer (Yunxi Analytical Instrument Factory, China), 5804R high-speed centrifuge (Eppendorf, Germany) were used in pharmacokinetic experiments. Yuexu Column was set Welch ultimate XB-C18, 2.1×100mm, 5μm; 2.1mm analytical column protection kit. Ponatinib (Meilun Biotechnology Co., Ltd., Dalian, China) is taken as the standard.

New Zealand White rabbits weighing 2.5–3 kg were purchased from the Animal Experimental Center of Huazhong University of Science and Technology. The Animal Experiment Committee of the Institute for Huazhong University of Science and Technology approved all experimental protocols. All animal experiments were performed in accordance with the National Institutes of Health Guidelines for the Care and Use of Laboratory Animals.

Study Design and Animal Model

A total of 65 VX2 tumor-burdened rabbits were randomly divided into five groups and treated transarterially with apatinib-loaded PIB (Group PA, 0.4 mL, n=13), PIB alone (Group P, 0.4 mL, n=13), iodized oil alone (Group I, 0.4 mL, n=13), apatinib solution (Group A, 0.4 mL, n=13) or saline (Group NS, 0.4 mL, n=13). The dose of apatinib (Hengrui Medicine Co., Jiangsu) was 2 mg/kg.

A 4-cm incision was made in the middle of the rabbit's abdominal cavity to expose the hepatic lobe. A 1-mm^3 piece of VX2 tumor tissue was imbedded into the left medial lobe of the liver to a depth of ~0.5 cm and covered with gelatin. On day 16 after implantation, the size of liver

tumors was measured by a contrast-enhanced CT scan, and rabbits with tumors ranging from 10 to 20 mm in diameter were selected for subsequent interventional embolization.

Interventional Therapy Process

All rabbits were anesthetized with an intraperitoneal injection of 2.5 mL/kg chloral hydrate. The femoral artery was isolated, and the 4F vascular sheath was catheterized. Hepatic arteriography was performed under the guidance of digital subtraction angiography (DSA), and a 2.7F microcatheter was super-selectively inserted into the tumor donor branch. Then, each group was treated with the corresponding embolization, and the blood supply of tumors was occluded and reconfirmed by post-embolization angiography. Next, the femoral artery was ligated after extubation. Finally, the incision was sterilized and sutured with gentamicin (20–40 thousand IU), and penicillin (0.2 million IU) was intramuscularly injected for 3 days to prevent infection.

Tissue Sample Harvesting

An enhanced CT scan was performed 1 day before and 7 days after surgery. Contrast-enhanced CT images were processed using the Syngo Fastview image processing system, and the shape, location, necrosis, size and intrahepatic metastasis of liver tumors were analyzed and recorded by two senior radiologists. The transverse diameter (D_t) and maximum diameter (D_m) of the tumors were recorded, and the tumor volumes were calculated according to the equation: $V=D_m \times D_t^2/2$. The preoperative volume (V0) and postoperative volume (V7) were measured, and the tumor growth rates in each group were calculated according to the formula: $V_7/V_0 \times 100$.

Five tumor-bearing rabbits were euthanized at 7 days after TAE in each group. The tumors and surrounding liver tissues were removed after dissection. The tumors were imaged, and the tumor length was re-measured. Tumors were fixed with formalin and embedded with paraffin to obtain specimens for immunohistochemical analysis, and smears were stained with hematoxylin and eosin (HE). The microvessel density (MVD) was measured and analyzed in the five groups of tumors at each time point. The remaining 40 tumor-bearing rabbits were monitored and recorded for survival time.

Pharmacokinetic Testing

Serum Treatment

We collected serum samples 0 min, 1 min, 5 min, 10 min, 30 min, 1 h, 2 h, 8 h, 24 h and 48 h after TAE for all groups. At each time point, blood samples were collected from each tumor-bearing rabbit through the ear vein and analyzed using an Agilent 1200 high-performance liquid chromatography (HPLC) system.

The supernatant was transferred to a 2-mL Eppendorf tube, and 50 μL of supernatant, 140 μL methanol and 10 μL Ponatinib (IS,1 μg/mL) were added to the precipitated pellet followed by vortex-mixing and centrifugation (at 2500 rpm for 3 min at 4°C and 14,000 rpm for 10 min at 4°C).

Liver Tissue Collection

We collected liver tissue samples 4 h, 1 d, 3 d, 10 d, 26 d and 36 d after treatment from all groups. The HCC center, adjacent cancer and surrounding cancer tissue specimens were fixed in formalin. Then, 100-mg tissue samples were harvested, added to 1 mL PBS, and placed into a KZ-II high-speed tissue grinder (Service bio, Wuhan Saiwell Biotechnology Co., Ltd., China) for sufficient grinding. Samples were centrifuged (1000 r/min, 5 min), and the supernatant was collected. The sample preparation method was the same as that for serum treatments.

Statistical Analysis

All data were expressed as the mean ± SD. All graphics were generated in GraphPad prism V8.0. The measurement data were statistically analyzed by a paired *t*-test and one-way ANOVA using SPSS version 20.0 software. The difference was statistically significant when the P-value <0.05.

Establishment of VX2 Tumor-Bearing Rabbit and Tumor Growth Rate Measurements

All rabbit VX2 tumor implantations and TAE procedures were performed successfully by the same operators. Enhanced CT scanning was performed on VX2 tumor-bearing rabbits 1 day before TAE treatment. We observed a mild low-density area in the left lobe of the liver and prominent necrosis in the central region of the tumor. There was a significant enhancement around the tumor, which had an average size of 1.66±0.14 cm × 1.50 ±0.12 cm (Figure 1A).

To verify the use of apatinib-loaded PIB nanogel for TAE therapy in HCC, TAE was performed in rabbits with implanted VX2 tumors (Figure 1B). The tumor growth rate was calculated 7 days after TAE in each group (Table 1, Figure 2C). The data showed that the tumor growth rate in Group PA was significantly lower than the other four groups (P=0.000<0.01).

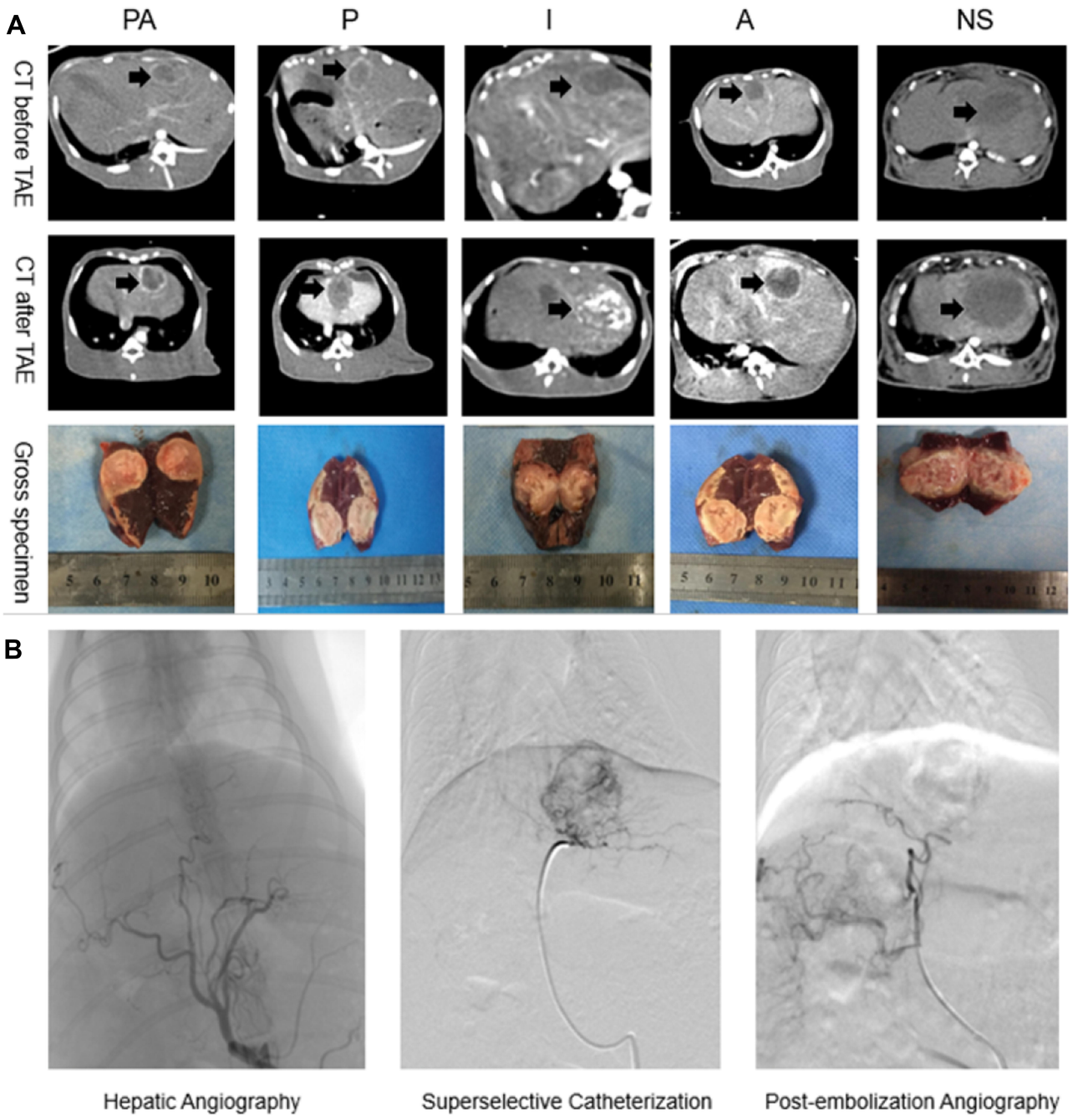

Figure 1 (**A**) Abdominal contrast-enhanced CT scan was performed on VX2 tumor-bearing rabbits before and after TAE. We could see the nearly-circular tumor in the left lobe of liver (black arrows). (**B**) Hepatic artery angiography of rabbit liver before embolization, then super-selective catheterization and administer by the group. Blood supply of tumor was occluded and reconfirmed by post-embolization angiography.

Further comparative analysis revealed that the tumor growth rate was reduced in Group PA compared with Groups P and I ($P=0.032<0.05$), and compared with Groups A and NS, Group PA showed more significant inhibition of tumor volume growth ($P=0.000<0.01$). Furthermore, the tumor growth rate was reduced in Group P compared with Group I ($P=0.0446<0.05$). No statistical difference was found between Groups A and NS ($P=0.0756>0.05$).

Immunohistochemical Examination Results

Gross liver specimens were harvested 7 days after TAE, and the images obtained showed that the tumor volume

Table 1 Volume Changes Before and After VX2 Tumor Interventional Therapy in the Five Groups

Group	Tumor Volume 1 Day Before TAE $V_1(cm^3)$	Tumor Volume 7 Days After TAE V_7 (cm^3)	Tumor Growth Rate $V_7/V_1 \times 100\%$
Group PA	1.90±0.50	2.21±0.66	115.38±6.04
Group P	1.89±0.34	2.67±0.47	143.43±12.89
Group I	1.85±0.38	2.80±0.53	152.23±17.85
Group A	1.92±0.37	4.07±0.55	214.10±12.10
Group NS	1.87±0.37	4.64±0.42	254.86±32.78
F value	0.019	14.660	37.230
P value	0.999	0.000	0.000

was increased than before, and accompanied by central and peripheral regional necrosis (Figure 1). Consistent with the gross specimens, the HE staining data revealed that Groups PA, P and I showed less residual cancer cells and larger tumor necrosis areas compared with Groups NS and A. Additionally, because CD31 expression is highly related to tumor angiogenesis, we examined the expression of CD31 by immunohistochemical staining as an indication of tumor MVD. The results showed that CD31 expression in Group PA was considerably lower than that of the other four groups (P=0.000<0.01), suggesting that TAE with apatinib-loaded PIB nanogels could inhibit tumor angiogenesis (Figure 2A and B). Furthermore, pairwise comparison results showed reduced CD31 expression in the tumor area in Group PA compared with Group P (P = 0.0312<0.05). Additionally, compared with Groups I, A and NS, Group PA exhibited more significant differences in CD31 expression in the tumor area (P=0.00<0.01).

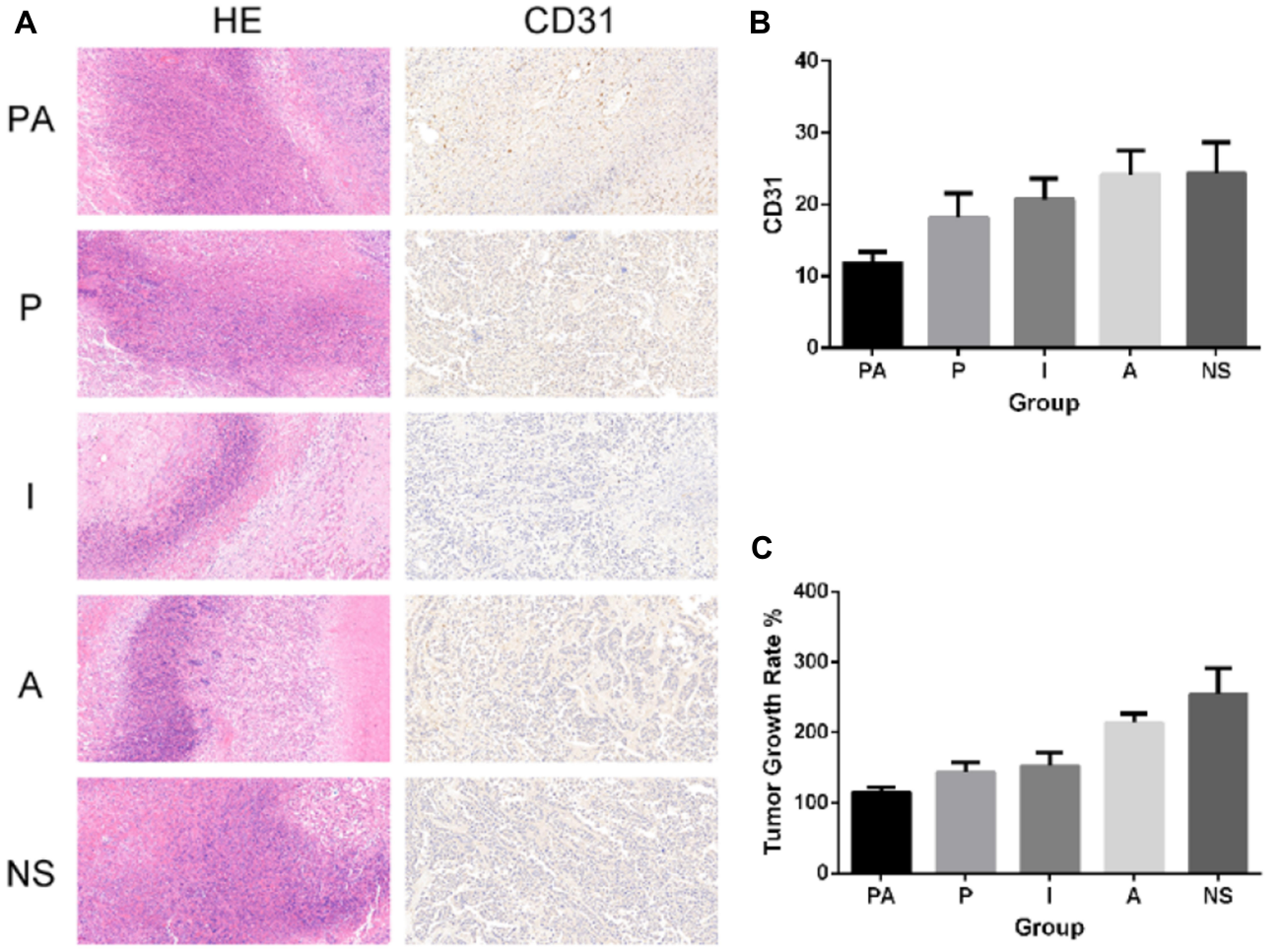

Figure 2 (**A**) Images of HE staining and CD31 staining of each group under light microscopy (200×), (**B**) CD31 count in liver tumor tissues. Apatinib substantially inhibited CD31, the CD31 of group PA was considerably lower than that of group P (P = 0.0312 <0.05). (**C**) Tumor growth rate of each group. The tumor growth rate of Group PA was markedly lower than the other four groups (P=0.000<0.01).

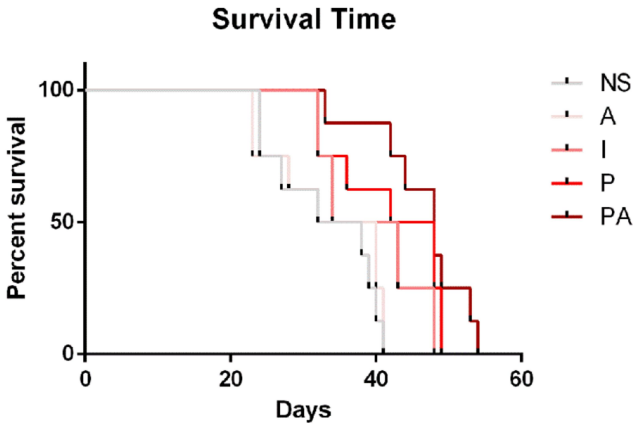

Figure 3 The survival time of tumor-burdened rabbits. The average survival time of Groups PA, P, I, A, and NS is 46.375±6.304, 42±7.124, 39.25±6.534, 33.5±7.5, and 33.125±6.827 days, respectively.

Survival Curve Analysis

The survival times of tumor-burdened rabbits were recorded and plotted as a survival curve (Figure 3). The average survival times in Groups PA, P, I, A and NS were 46.375±6.304, 42±7.124, 39.25±6.534, 33.5±7.5 and 33.125±6.827 days, respectively. We found a significant difference in survival time among the five groups, and the survival time of tumor-burdened rabbits was significantly prolonged in the PA group (P=0.000<0.01).

Consistent with the tumor growth rate, further pairwise comparisons revealed that the survival time of tumor-burdened rabbits in Group PA was markedly longer than that in Group P (P=0.0106<0.05). Moreover, compared with Groups A and NS, Group PA showed more significant inhibition of the tumor volume growth rate (P=0.000<0.01). Reduced tumor growth rates were also observed in Group P compared with Group I (P=0.0321<0.05). No statistical difference was found between Groups A and NS (P=0.3506>0.05).

Pharmacokinetics

Apatinib levels were measured in serum samples collected at 0 min, 1 min, 5 min, 10 min, 30 min, 1 h, 2 h, 8 h, 24 h and 48 h after TAE by HPLC. The concentration of apatinib in the serum declined over time after TAE (Figure 4). The administration of apatinib by TAE with apatinib-loaded PIB nanogel resulted in apatinib concentrations of 0 ±0 ng/mL, 51.03±8.53 ng/mL, 20.10±6.80 ng/mL, 9.06 ±3.02 ng/mL, 6.46±0.35 ng/mL, 5.91±0.66 ng/mL, 3.46 ±1.34 ng/mL, 0.79±0.011 ng/mL, 0.14±0.047 ng/mL and 0 ±0 ng/mL in the peripheral blood at 0 min, 1 min, 5 min, 10 min, 30 min, 1 h, 2 h, 8 h, 24 h and 48 h, respectively, after TAE (Figure 4A).

Tumor-burdened rabbits were euthanized, liver samples were collected 4 h, 1 d, 3 d, 10 d, 26 d and 36 d after TAE, and the apatinib concentrations in the HCC center, adjacent cancer and periphery tissue specimens were determined. The apatinib concentration in the liver tissue decreased over time after TAE. The administration of apatinib by TAE with apatinib-loaded PIB nanogels resulted in apatinib concentrations of 206.57±60.87 ng/mL, 157.03±44.09 ng/mL, 138.40±81.60 ng/mL, 11.40 ±3.27 ng/mL, 10.31±3.52 ng/mL and 3.33±0.82 ng/mL in the HCC center at 4 h, 1 d, 3 d, 10 d, 26 d and 36 d, respectively, after TAE. The apatinib concentrations in the adjacent cancer were 673.00±130.64 ng/mL, 298.33

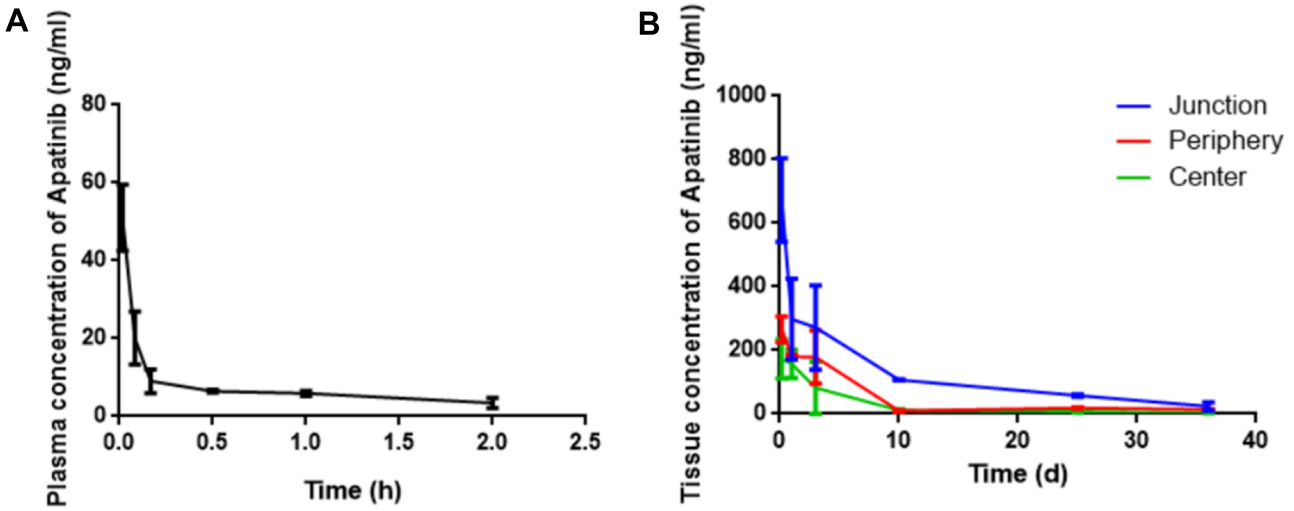

Figure 4 (**A**) The plasma concentration curves of apatinib after TAE (n=3). (**B**) The tissue concentration curves of apatinib after TAE (n=3).

±127.05 ng/mL, 272±132.83 ng/mL, 107.18±0.59 ng/mL, 58.17±4.17 ng/mL and 23.44±13.10 ng/mL at 4 h, 1 d, 3 d, 10 d, 26 d and 36 d, respectively, after TAE. In addition, the apatinib concentrations in the periphery were 266.00 ±40.42 ng/mL, 251.00±6.13 ng/mL, 179.40±83.96 ng/mL, 54.23±2.07 ng/mL, 18.67±1.72 ng/mL and 13.90±0.82 ng/mL at 4 h, 1 d, 3 d, 10 d, 26 d and 36 d, respectively, after TAE (Figure 4B).

The apatinib concentration in the blood fell to below 10 ng/mL within 10 min after TAE and dropped below 1 ng/mL after 8 h. The drug was released continuously into the liver for 36 days, with the highest concentration at the tumor junction ($P=0.045<0.05$).

Discussion

The limited postoperative effect of TAE and the metastasis and recurrence of HCC are considered to be closely related to the highly hypoxic microenvironment induced by TAE.[48,49] Thus, the development of new embolic materials to prevent tumor recurrence and metastasis after TAE is essential for the effective interventional treatment of HCC. Compared with lipiodol, PIB has the advantage of controlling the level of occlusion and drug release. The goal of using TAE with apatinib-loaded PIB nanogel was to provide sustained and prolonged drug delivery and high diffusion of apatinib in the liver tissue around the tumor. Currently, there is no report on the application of TAE with apatinib-loaded PIB nanogel as an interventional therapy for HCC. Therefore, we propose a novel concept of TAE with apatinib-loaded PIB for the targeted treatment of HCC. The results show that this new dosing regimen successfully prevented the growth and recurrence of VX2 tumors and prolonged the survival time of VX2 tumor-bearing rabbits.

Angiogenesis is necessary for tumor invasion and migration and is an essential characteristic of tumor development.[11] As the hypoxic environment after TAE has been increasingly recognized, experts have investigated new approaches for vascular normalization in HCC.[50] Therefore, the anti-angiogenic effect of TAE with apatinib-loaded PIB nanogels was explored in this study. The analysis of tumor growth rates and MVD verified that there were considerable differences between Groups PA and P. The data showed that TAE with apatinib-loaded PIB achieved a more substantial inhibition of MVD and tumor growth rate in the VX2 tumor-bearing rabbits than PIB alone, suggesting that apatinib plays a role in preventing tumor growth by inhibiting tumor angiogenesis. We also observed that the survival time of VX2 tumor-bearing rabbits in Group PA was significantly longer than that in Group P. Comprehensively, our results revealed that TAE with apatinib-loaded PIB nanogel has great potential as a pharmaceutical treatment for human HCC by inhibiting angiogenesis.

Traditional interventional chemoembolization involves mixing antitumor drugs with lipiodol and injecting this mixture into the hepatic artery with or without other embolic materials, such as gelatin sponges and PVA. However, the properties and stability are quite different, and this approach fails to generate a controlled release model.[51–53] It is interesting that the apatinib only TAE approach was irrelevant to tumor control and survival. This result indicates that transient perfusion chemotherapy is not effective and the importance of embolization materials in interventional therapy of HCC. With the development of interventional radiology and polymer materials, the identification of new drug-carrying embolization materials has become a topic of high interest.[54–56] At present, research on interventional embolization materials for HCC mainly focuses on the preparation of drug-eluting microspheres.[57,58] Although drug-eluting microspheres transarterial chemoembolization shows a specific slow-release effect, it does not last long. The drug in the liver decreased to minimal levels (less than 10 ng/mL) within 2 weeks to 1 month after the operation.[59,60]

Because PIB nanogel is a cross-linked interpenetrating network polymer with a size of 10–1000 nm, a variety of bioactive molecules can be embedded in its three-dimensional mesh structure. Following targeted drug delivery through TAE surgery, the drug is gradually released from the three-dimensional network structure to achieve the controlled release of the drug. The results of the present study showed that a high concentration of apatinib persists in the liver for 36 days. The analysis of tissue pharmacokinetics indicates that PIB has a potent sustained-release effect, and the apatinib concentration is highest at the edge of the tumor where it exerts its antitumor and anti-angiogenic effects. The tumor center had the lowest drug concentration because it lacked blood supply, thereby preventing drug access. The tumor margin is the area most likely to remain and relapse after interventional embolization. Thus, we concluded that TAE with apatinib-loaded PIB nanogel provides high concentrations of apatinib that continuously act on the margins of HCC and inhibit tumor growth to

achieve a lasting effect. Consequently, TAE with apatinib-loaded PIB is an effective strategy.

The results of this study also revealed that apatinib reaches a relatively high concentration in the plasma within a short period after TAE. However, apatinib concentrations in the blood drop below 10 ng/mL within 10 min and are almost undetectable at 48 h. The plasma pharmacokinetic results provide evidence that this treatment can potentially reduce systemic side effects, which is a crucial factor contributing to poor patient compliance. Compared with conventional TACE with oral apatinib, TAE with apatinib-loaded PIB nanogels allows permanent embolization of blood vessels, provides a slow continuous release of antitumor drugs in a locally targeted manner and reduces the systemic release of antitumor drugs, thereby significantly decreasing the adverse effects.[61]

Apatinib-loaded PIB nanogels can be used as an active liquid embolic material for interventional therapy in VX2 tumor-bearing rabbits. apatinib is targeted to the margins of HCC tissues through PIB nanogels, which achieve a slow and sustained release of the drug in the tumor and significantly reduced systemic drug concentrations. Further experiments showed significantly prolonged survival times and an inhibitory effect on tumor growth. This study is expected to provide new targets and therapeutic strategies for the interventional treatment of HCC, and our approach has great application potential.

Abbreviations

HCC, hepatic carcinoma; PIB, poly(*N*-isopropylacrylamide-*co*-butyl methyl acrylate) temperature-sensitive; TAE, transcatheter arterial embolization; MVD, microvessel density; VEGF, vascular endothelial growth factor; VEGFR, vascular endothelial growth factor receptor; CT, computed tomography; DSA, digital subtraction angiography.

Acknowledgments

This work was financially supported by grants from National Natural Science Foundation of China (grant No. 81873917 and 81471766). We are grateful to the Animal Center, the Department of central laboratory of Wuhan Union Hospital, Tongji Medical College, Huazhong University of Science and Technology.

Disclosure

The authors have declared that no competing interest exists.

References

1. Chen W, Zheng R, Baade PD, et al. Cancer statistics in China, 2015. *CA Cancer J Clin*. 2016;66(2):115–132. doi:10.3322/caac.21338
2. Petrick JL, Kelly SP, Altekruse SF, et al. Future of hepatocellular carcinoma incidence in the United States forecast through 2030. *J Clin Oncol*. 2016;34(15):1787–1794. doi:10.1200/JCO.2015.64.7412
3. Bray F, Ferlay J, Soerjomataram I, et al. Global cancer statistics 2018: GLOBOCAN estimates of incidence and mortality worldwide for 36 cancers in 185 countries. *CA Cancer J Clin*. 2018;68(6):394–424. doi:10.3322/caac.21492
4. Llovet JM, Bruix J. Systematic review of randomized trials for unresectable hepatocellular carcinoma: chemoembolization improves survival. *Hepatology*. 2003;37(2):429–442. doi:10.1053/jhep.2003.50047
5. Xiao EH, Guo D, Bian DJ. Effect of preoperative transcatheter arterial chemoembolization on angiogenesis of hepatocellular carcinoma cells. *World J Gastroenterol*. 2009;15(36):4582–4586. doi:10.3748/wjg.15.4582
6. Llovet JM, Ricci S, Mazzaferro V, et al. Sorafenib in advanced hepatocellular carcinoma. *N Engl J Med*. 2008;359(4):378–390. doi:10.1056/NEJMoa0708857
7. Zhu AX, Duda DG, Sahani DV, et al. HCC and angiogenesis: possible targets and future directions. *Nat Rev Clin Oncol*. 2011;8(5):292–301. doi:10.1038/nrclinonc.2011.30
8. Feng GS. Conflicting roles of molecules in hepatocarcinogenesis: paradigm or paradox. *Cancer Cell*. 2012;21(2):150–154. doi:10.1016/j.ccr.2012.01.001
9. Carmeliet P, Jain RK. Molecular mechanisms and clinical applications of angiogenesis. *Nature*. 2011;473(7347):298–307.
10. Palazon A, Tyrakis PA, Macias D, et al. An HIF-1alpha/VEGF-A axis in cytotoxic T cells regulates tumor progression. *Cancer Cell*. 2017;32(5):669–683.e665. doi:10.1016/j.ccell.2017.10.003
11. Li J, Xu Y, Long XD, et al. Cbx4 governs HIF-1alpha to potentiate angiogenesis of hepatocellular carcinoma by its SUMO E3 ligase activity. *Cancer Cell*. 2014;25(1):118–131. doi:10.1016/j.ccr.2013.12.008
12. Simon T, Gagliano T, Giamas G. Direct effects of anti-angiogenic therapies on tumor cells: VEGF signaling. *Trends Mol Med*. 2017;23(3):282–292. doi:10.1016/j.molmed.2017.01.002
13. Kim KL, Suh W. Apatinib, an inhibitor of vascular endothelial growth factor receptor 2, suppresses pathologic ocular neovascularization in mice. *Invest Ophthalmol Vis Sci*. 2017;58(9):3592–3599. doi:10.1167/iovs.17-21416
14. Kaseb AO, Morris JS, Hassan MM, et al. Clinical and prognostic implications of plasma insulin-like growth factor-1 and vascular endothelial growth factor in patients with hepatocellular carcinoma. *J Clin Oncol*. 2011;29(29):3892–3899. doi:10.1200/JCO.2011.36.0636
15. Vasudev NS, Reynolds AR. Anti-angiogenic therapy for cancer: current progress, unresolved questions and future directions. *Angiogenesis*. 2014;17(3):471–494.
16. Ellis LM, Hicklin DJ. VEGF-targeted therapy: mechanisms of anti-tumour activity. *Nat Rev Cancer*. 2008;8(8):579–591. doi:10.1038/nrc2403
17. Peng QX, Han YW, Zhang YL, et al. Apatinib inhibits VEGFR-2 and angiogenesis in an in vivo murine model of nasopharyngeal carcinoma. *Oncotarget*. 2017;8(32):52813–52822. doi:10.18632/oncotarget.17264
18. Ferrara N, Gerber HP, Lecouter J. The biology of VEGF and its receptors. *Nat Med*. 2003;9(6):669–676. doi:10.1038/nm0603-669
19. Viallard C, Larrivee B. Tumor angiogenesis and vascular normalization: alternative therapeutic targets. *Angiogenesis*. 2017;20(4):409–426. doi:10.1007/s10456-017-9562-9

20. Thomas MB, Morris JS, Chadha R, et al. Phase II trial of the combination of bevacizumab and erlotinib in patients who have advanced hepatocellular carcinoma. *J Clin Oncol*. 2009;27(6):843–850. doi:10.1200/JCO.2008.18.3301
21. Kelley RK, Verslype C, Cohn AL, et al. Cabozantinib in hepatocellular carcinoma: results of a Phase 2 placebo-controlled randomized discontinuation study. *Ann Oncol*. 2017;28(3):528–534. doi:10.1093/annonc/mdw651
22. Liapi E, Geschwind JF. Combination of local transcatheter arterial chemoembolization and systemic anti-angiogenic therapy for unresectable hepatocellular carcinoma. *HCC*. 2012;1(3–4):201–215.
23. Kudo M, Imanaka K, Chida N, et al. Phase III study of sorafenib after transarterial chemoembolisation in Japanese and Korean patients with unresectable hepatocellular carcinoma. *Eur J Cancer*. 2011;47(14):2117–2127. doi:10.1016/j.ejca.2011.05.007
24. Lencioni R, Llovet JM, Han G, et al. Sorafenib or placebo plus TACE with doxorubicin-eluting beads for intermediate stage HCC: the SPACE trial. *J Hepatol*. 2016;64(5):1090–1098. doi:10.1016/j.jhep.2016.01.012
25. Kudo M, Han G, Finn RS, et al. Brivanib as adjuvant therapy to transarterial chemoembolization in patients with hepatocellular carcinoma: a randomized phase III trial. *Hepatology*. 2014;60(5):1697–1707. doi:10.1002/hep.27290
26. Kudo M, Ueshima K, Torimura T, et al. Randomized, open label, multicenter, phase II trial of transcatheter arterial chemoembolization (TACE) therapy in combination with sorafenib as compared with TACE alone in patients with hepatocellular carcinoma: TACTICS trial. *J Clin Oncol*. 2018;36(15):1.
27. Tian S, Quan H, Xie C, et al. YN968D1 is a novel and selective inhibitor of vascular endothelial growth factor receptor-2 tyrosine kinase with potent activity in vitro and in vivo. *Cancer Sci*. 2011;102(7):1374–1380. doi:10.1111/j.1349-7006.2011.01939.x
28. Roviello G, Ravelli A, Polom K, et al. Apatinib: a novel receptor tyrosine kinase inhibitor for the treatment of gastric cancer. *Cancer Lett*. 2016;372(2):187–191. doi:10.1016/j.canlet.2016.01.014
29. Fan M, Zhang J, Wang Z, et al. Phosphorylated VEGFR2 and hypertension: potential biomarkers to indicate VEGF-dependency of advanced breast cancer in anti-angiogenic therapy. *Breast Cancer Res Treat*. 2014;143(1):141–151. doi:10.1007/s10549-013-2793-6
30. Peng S, Zhang Y, Peng H, et al. Intracellular autocrine VEGF signaling promotes EBDC cell proliferation, which can be inhibited by Apatinib. *Cancer Lett*. 2016;373(2):193–202. doi:10.1016/j.canlet.2016.01.015
31. Li J, Zhao X, Chen L, et al. Safety and pharmacokinetics of novel selective vascular endothelial growth factor receptor-2 inhibitor YN968D1 in patients with advanced malignancies. *BMC Cancer*. 2010;10:529. doi:10.1186/1471-2407-10-529
32. Li J, Qin S, Xu J, et al. Apatinib for chemotherapy-refractory advanced metastatic gastric cancer: results from a randomized, placebo-controlled, parallel-arm, phase II trial. *J Clin Oncol*. 2013;31(26):3219–3225. doi:10.1200/JCO.2013.48.8585
33. Ding L, Li QJ, You KY, et al. The use of apatinib in treating nonsmall-cell lung cancer: case report and review of literature. *Medicine (Baltimore)*. 2016;95(20):e3598. doi:10.1097/MD.0000000000003598
34. Turjman F, Massoud TF, Vinters HV, et al. Collagen microbeads: experimental evaluation of an embolic agent in the rete mirabile of the swine. *AJNR Am J Neuroradiol*. 1995;16(5):1031–1036.
35. Sniderman KW, Sos TA, Alonso DR. Transcatheter embolization with Gelfoam and Avitene: the effect of Sotradecol on the duration of arterial occlusion. *Invest Radiol*. 1981;16(6):501–507. doi:10.1097/00004424-198111000-00009
36. Davidson GS, Terbrugge KG. Histologic long-term follow-up after embolization with polyvinyl alcohol particles. *AJNR Am J Neuroradiol*. 1995;16(4 Suppl):843–846.
37. Dhaliwal SK, Annamalai G, Gafoor N, et al. Portal vein embolization: correlation of future liver remnant hypertrophy to type of embolic agent used. *Can Assoc Radiol J*. 2018;69(3):316–321. doi:10.1016/j.carj.2018.02.003
38. Iwazawa J, Ohue S, Hashimoto N, et al. Local tumor progression following lipiodol-based targeted chemoembolization of hepatocellular carcinoma: a retrospective comparison of miriplatin and epirubicin. *Cancer Manag Res*. 2012;4:113–119. doi:10.2147/CMAR.S30431
39. Konno T, Maeda H, Yokoyama I, et al. [Use of a lipid lymphographic agent, lipiodol, as a carrier of high molecular weight antitumor agent, smancs, for hepatocellular carcinoma]. *Gan to Kagaku Ryoho*. 1982;9(11):2005–2015. Japanese.
40. Choi JW, Cho HJ, Park JH, et al. Comparison of drug release and pharmacokinetics after transarterial chemoembolization using diverse lipiodol emulsions and drug-eluting beads. *PLoS One*. 2014;9(12):e115898. doi:10.1371/journal.pone.0115898
41. Nouri YM, Kim JH, Yoon HK, et al. Update on transarterial chemoembolization with drug-eluting microspheres for hepatocellular carcinoma. *Korean J Radiol*. 2019;20(1):34–49. doi:10.3348/kjr.2018.0088
42. Sluzewski M, Van Rooij WJ, Lohle PN, et al. Embolization of meningiomas: comparison of safety between calibrated microspheres and polyvinyl-alcohol particles as embolic agents. *AJNR Am J Neuroradiol*. 2013;34(4):727–729. doi:10.3174/ajnr.A3311
43. Lewis AL, Gonzalez MV, Leppard SW, et al. Doxorubicin eluting beads - 1: effects of drug loading on bead characteristics and drug distribution. *J Mater Sci Mater Med*. 2007;18(9):1691–1699. doi:10.1007/s10856-007-3068-8
44. Jones RP, Dunne D, Sutton P, et al. Segmental and lobar administration of drug-eluting beads delivering irinotecan leads to tumour destruction: a case-control series. *HPB (Oxford)*. 2013;15(1):71–77. doi:10.1111/j.1477-2574.2012.00587.x
45. Neves AR, Queiroz JF, Weksler B, et al. Solid lipid nanoparticles as a vehicle for brain-targeted drug delivery: two new strategies of functionalization with apolipoprotein E. *Nanotechnology*. 2015;26(49):495103. doi:10.1088/0957-4484/26/49/495103
46. Zhao H, Zheng C, Feng G, et al. Temperature-sensitive poly (N-isopropylacrylamide-co-butyl methylacrylate) nanogel as an embolic agent: distribution, durability of vascular occlusion, and inflammatory reactions in the renal artery of rabbits. *AJNR Am J Neuroradiol*. 2013;34(1):169–176. doi:10.3174/ajnr.A3177
47. Qian K, Ma Y, Wan J, et al. The studies about doxorubicin-loaded p (N-isopropyl-acrylamide-co-butyl methylacrylate) temperature-sensitive nanogel dispersions on the application in TACE therapies for rabbit VX2 liver tumor. *J Control Release*. 2015;212:41–49. doi:10.1016/j.jconrel.2015.06.013
48. Saharinen P, Eklund L, Pulkki K, et al. VEGF and angiopoietin signaling in tumor angiogenesis and metastasis. *Trends Mol Med*. 2011;17(7):347–362. doi:10.1016/j.molmed.2011.01.015
49. Xu W, Kwon JH, Moon YH, et al. Influence of preoperative transcatheter arterial chemoembolization on gene expression in the HIF-1alpha pathway in patients with hepatocellular carcinoma. *J Cancer Res Clin Oncol*. 2014;140(9):1507–1515. doi:10.1007/s00432-014-1713-4
50. Zhou C, Yao Q, Zhang H, et al. Combining transcatheter arterial embolization with iodized oil containing apatinib inhibits HCC growth and metastasis. *Sci Rep*. 2020;10(1):2964. doi:10.1038/s41598-020-59746-1
51. Llovet JM, Real MI, Montaña X, et al. Arterial embolisation or chemoembolisation versus symptomatic treatment in patients with unresectable hepatocellular carcinoma: a randomised controlled trial. *Lancet*. 2002;359(9319):1734–1739. doi:10.1016/S0140-6736(02)08649-X
52. Deng G, Zhao DL, Li GC, et al. Combination therapy of transcatheter arterial chemoembolization and arterial administration of antiangiogenesis on VX2 liver tumor. *Cardiovasc Intervent Radiol*. 2011;34(4):824–832. doi:10.1007/s00270-011-0179-x

53. Tzeng WS, Wu RH, Chang SC, et al. Ionic versus nonionic contrast media solvents used with an epirubicin-based agent for transarterial chemoembolization of hepatocellular carcinoma. *J Vasc Interv Radiol*. 2008;19(3):342–350. doi:10.1016/j.jvir.2007.10.021
54. Mouli SK, Tyler P, Mcdevitt JL, et al. Image-guided local delivery strategies enhance therapeutic nanoparticle uptake in solid tumors. *ACS Nano*. 2013;7(9):7724–7733. doi:10.1021/nn4023119
55. Bedouet L, Verret V, Louguet S, et al. Anti-angiogenic drug delivery from hydrophilic resorbable embolization microspheres: an in vitro study with sunitinib and bevacizumab. *Int J Pharm*. 2015;484(1–-2):218–227. doi:10.1016/j.ijpharm.2015.02.039
56. Chen H, Gu Y, Hub Y, et al. Characterization of pH- and temperature-sensitive hydrogel nanoparticles for controlled drug release. *PDA J Pharm Sci Technol*. 2007;61(4):303–313.
57. Malagari K, Pomoni M, Moschouris H, et al. Chemoembolization of hepatocellular carcinoma with HepaSphere 30–60 mum. Safety and efficacy study. *Cardiovasc Intervent Radiol*. 2014;37(1):165–175. doi:10.1007/s00270-013-0777-x
58. Wang Y, Benzina A, Molin DG, et al. Preparation and structure of drug-carrying biodegradable microspheres designed for transarterial chemoembolization therapy. *J Biomater Sci Polym Ed*. 2015;26(2):77–91. doi:10.1080/09205063.2014.982242
59. Zhang S, Huang C, Li Z, et al. Comparison of pharmacokinetics and drug release in tissues after transarterial chemoembolization with doxorubicin using diverse lipiodol emulsions and CalliSpheres Beads in rabbit livers. *Drug Deliv*. 2017;24(1):1011–1017. doi:10.1080/10717544.2017.1344336
60. Hong K, Khwaja A, Liapi E, et al. New intra-arterial drug delivery system for the treatment of HCC: preclinical assessment in a rabbit model of HCC. *Clin Cancer Res*. 2006;12(8):2563–2567. doi:10.1158/1078-0432.CCR-05-2225
61. Shao F, Zhang H, Yang X, et al. Adverse events and management of apatinib in patients with advanced or metastatic cancers: a review. *Neoplasma*. 2020;67(4):715–723. doi:10.4149/neo_2020_190801N701